Study of the Liesegang Chemical Effects in Antique Bronze Artefacts During Their Stay Within an Archaeological Site

ION SANDU[1,2*], OTILIA MIRCEA[3], ANDREI VICTOR SANDU[2,4], VIORICA VASILACHE[1], IOAN GABRIEL SANDU[2,4*]

[1] Alexandru Ioan Cuza University of Iasi, Arheoinvest Platform, Laboratory for Scientific Investigation, 11 Carol I Blvd.,700506,Iasi, Romania

[2] Romanian Inventors Forum, 3 Sf. Petru Movila Str. Bl. L11, Sc. III, Et. 3, Ap.3, 700089, Iasi, Romania

[3] Roman History Museum, 19 Cuza Vodă, 611009, Roman, România

[4] Gheorghe Asachi Technical University of Iasi, Faculty of Materials Science and Engineering, 41A D. Mangeron, 700050, Iasi, Romania

Our paper presents various forms in which the processes of deterioration-degradation manifest on the surface and in the 3D spatial distribution of the metallic core and the corrosion bulk for a series of recently discovered archaeological items. In that regard, we paid special attention to the items with and without a metallic core, that presented the Liesegang effect, so as to elucidate the formation mechanisms thereof during the period before abandonment until their uncovering in the archaeological site. By stereo-microscopic analysis and by SEM-EDX, we established that both the metallic core and each Liesegang layer had a gradual composition with a radial disposition, from center to surface. The items that had a conserved metallic core, the concentration of Sn increased from the center of the core to the exterior, where it exceeded the normal limits of common antique bronze items. Nevertheless, the completely corroded items, without a metallic core, presented a black-gray compound in their center, which contained a significant amount of metallic tin, heavily diluted in copper and the external Liesegang layers were disposed in line with a congruent coating formed of tin and chloride ions and also a small and variable quantity of copper (much lower than that from the basic alloy). On top of that coating there formed the mineralized layers of cuprite, malachite, azurite, nantokite, atacamite, paratacamite etc., which formed by osmosis on passing through membranes of hydrogels from Sn, Pb and Zn oxyhydroxides, or from phosphoapatites. The morphology and distribution of those layers was dictated by the initial form of the item, by the processed used for its manufacture, by the conservation state thereof before abandonment, by the chemistry and pedology of the soil it lays in.

Keywords: ancient bronze, Liesegang effect, primary, secondary and contamination patina, OM, SEM-EDX

The bronze items discovered in recent years present a layered structure of the corrosion crusts, very clearly distinguishable in a transversal section, also known as the Liesegang effect [1-4]. Most of those layered structures are disposed concentrically around the metallic core, irrespective of the conservation state thereof, often extending continuously in the volume phase of the corrosion bulk.

In certain items which were uncovered in sites under specific aggressive conditions, the Liesegang effect was disposed zonally or radially, continuously, or interrupted by profound cracks reaching the metallic core. Others featured layered structures extending in honeycomb patters, only the membrane skeletons being identified, totally lacking any Liesegang congruent content resulted during underground stay [1, 2, 5-10].

By analyzing a large group of antique bronze items uncovered in various sites, we observed that the Lisegang effect manifested differently as regards its extent, manner of stratification and disposition, according to the composition of the basic alloy, to the nature of the primary patina and the state of conservation on abandonment, to the conditions in which the item stood buried and the aggressiveness of the soil [1, 2, 11-14].

Moreover, we also analyzed items with Liesegang structures that were disturbed by pedologic processes or by physico-mechanical disturbances in the burial area, but by sequential analysis we managed to identify the compounds in the three patinas: *the primary,* or *noble patina, the secondary,* or *poor patina and the tertiary,* or *contamination patina* [1-6, 15-30].

The formation mechanism of the Liesegang layers on bronze items has not yet been completely clarified.

We know that bronzes which contain Sn, Pb and Zn, due to their shifting to a cationic form in moist environments with cyclical variations in their condition, display the Liesegang phenomenon, which is caused by the coatings of Sn(IV), Pb(II) and/or Zn(II) hydrogels and, in the case of soils rich in phosphates, those coatings from chloride- or hydroxy-apatites may trigger a layered recrystallization of the compounds from the first two patinas, by direct and inverse osmoses.

In highly aggressive soil conditions and in pedologically disturbed sites some items form the tertiary, or contamination patina, as a series of new structures, which may continuously consume the metallic core and may include into the corrosion crust certain minerals, organic or inorganic materials from the surroundings. Whereas certain organic materials that get included in the bulk are conserved under the action of the antibiotic cations from the corrosion products, in time, other materials suffer processes of mineralization and fossilization [2, 15, 16, 19-30].

According to the cyclical environmental conditions, but also to the complexity of the structural elements of an item (bolts, fillings, coatings, weldings etc.) the Liesegang effect may cover the entire item, or only parts thereof. It evolves according to the shape and complexity of the item,

* *email: ion.sandu@uaic.ro, gisandu@yahoo.com*

to the composition of the alloy and the surrounding environment, to the manufacturing processes, or thermal processes to which the item was subject after its abandonment (fires, arson etc.) and to the seasonal temperature cycles.

As mentioned before, the Liesegang layers are based on coating membranes of hydrogels, which are prone to direct and micro-porous membrane osmoses, based on hydroxy- or chloride-apatites, both of which have a specific permeability to certain cations and anions.

In both cases, while shifting from moist gel-forming environments to dry, sicativating environments, those structures may recrystallize in layers, in a specific order of the compounds from the first two patinas, such as: cuprite, chalcocite, nantokite, atacamite, paratacamite, malachite, azurite etc.

The stratification mode, the nature of the coating agent and the extent of the Liesegang effect are often used as important archaeometric characteristics in authentication and to establish the evolution of an item from manufacture to discovery, especially to establish the context in which it was used and that of its abandonment [15,16, 19-30].

Our paper presents a series of Liesegang effects, manifesting differently as regards their stratification, the nature of the coating agent and the extent of the effect, on certain bronze items recently discovered in Romania, which were analyzed on the surface and in section by OM and SEM-EDX.

The Evolution of the Corrosion Structures in Bronze Artifacts from Manufacture to Extraction from the Archaeological Site

Ancient bronze items from archaeological sites contain in their corrosion crust, or in their bulk, a series of basic chemical components, specific to the three periods:

- manufacture and use;
- abandonment and
- underground stay.

Those compounds may by grouped into *primary, secondary and tertiary patinas,* the first two being surface patinas and the third residing in the volume phase of the bulk [1-6].

The primary patina, also known as *noble patina* [1, 7, 15, 16] due to its aesthetic and protective function, forms during the manufacture period and the first part of the use period when, by purely chemical and electro-chemical redox processes, there form thin continuous coatings, initially from oxides and sulfurs of Cu(I, II), which have a significant protective and aesthetic role. The formation of that patina is mainly based on the oxygen in the air, the sulfide and the sulfureated hydrogen resulted from the cystin and cystein of the skin that comes in contact with the object during use [15-30].

Towards the end of the use period, Cu (II) basic carbonates form over the cuprite coating, out of which only the *malachite* functions as a protective and aesthetic, noble patina, the *azurite* leading to crystallites, or to lumps with very different morphologies that are prone to undergo processes of dissolution and to form other compounds [1, 2, 5-11].

Those coatings, appearing as even monochrome or polychrome surfaces, uniform and compact, may contain randomly distributed small areas with uneven structures, especially on items found in aggressive environments. Those surfaces may have colors specific to primary patina compounds (brown-red, green, gray), but also secondary patina colors (blue, green, brown, red, bright to dark gray) with an even and bright appearance. Among those compounds that form such thin, uniform and compact coatings, the main ones are Cu(I and II) compounds, with O^{2-} and S^{2-} anions, which subsequently form complex Cu(II) chloride-hydroxy compounds, which are prone to form green-gray glossy, protective malachite ($Cu_2(OH)_2CO_3$) coatings, in alkaline environments and in the presence of CO_2.

The even, primary patina coatings on very old items may often contain cracks and pits caused by physical and mechanical stresses. Thermal stresses (fires, arson, ritual burning etc.) may form networks of intergranulary, or transgranulary cracks which, by corrosion, deepen and may have profound evolutionary effects.

Moreover, iridescent surfaces with patterns of microtextures are also part of the group of surface deteriorations, which appear when an item is subject to processes of erosion under the action of waters with debris (sand, gravel etc.), both from surface water sources (rivers, waves) and from underground ones. Iridescence and texture patterns may also result after landslides, land formation activities, excavations and agricultural activities. Such situations may often generate serious damage to items, such as: flattening, bending, twisting, piercing, scratching, tearing, breaking etc.

The secondary patina appears during the final period of use, under the influence of factors from aggressive environments which, after competitive processes: redox and complexation, assisted by acid-bases, in the presence of the chloride anion in an acid environment, but also of oxygen and carbon dioxide in an alkaline environment. They lead to the formation of corrosion structures with various 3D dispositions. First forms the *nantokite* (CuCl) and its alkaline forms: *atacamite* ($Cu_2Cl(OH)_3$ – orthorhombic, hydrated form)/*paratacamite* ($Cu_2(OH)_3Cl$ – rhombohedral, anhydric form), then, by Liesegang effect, forms the *cuprite* (Cu_2O), the *malachite* ($Cu_2(OH)_2CO_3$)/*the azurite* ($Cu_3(OH)_2(CO_3)_2$) and *ceruzite* ($Pb_2(OH)_2CO_3$) layer and after that the *chalconite* ($CuSO_4 \times 5H_2O$), *antlerite* ($Cu_3(OH)_4SO_4$), *brocantite* ($Cu_4(OH)_6SO_4$) *and/or langite* ($Cu_4(OH)_6SO_4 \times H_2O$), together with *casiterite* (SnO_2), *zincite* (ZnO) etc. The above are distributed unevenly on the surface of the item, with only a few small even areas, protected or not. Those processes are often disturbed right before the abandonment period and during the underground stay, by the formation of lumps and bulbs, shaped as profound "carbuncles" that penetrate the primary patina, reaching the metallic core through the cracks and fine orifices produced by the pitting corrosion, which then form cracks and pits, by contraction and dissolution [1, 2, 5, 6, 8, 10-26].

The secondary patina, in contrast to the primary one that is of a ceram-calcogenic type, shaped as an even and continuous protective coating, forms under the influence of the chloride anion, in atmospheres with an excess of CO_2, or in the presence of the anions HCO_3^-, CO_3^{2-} or SO_4^{2-}. Initially, the chloride anion activates the cuprite or chalcolite, penetrates under the primary patina, where it forms natochite and the hydrated forms of atacamite and the anhydrous ones of paratacamite.

In the absence of the chloride anion from environments hydrated with CO_2, malachite ($Cu_2(OH)_2CO_3$) forms on top of the primary patina as a thin, uniform, protective monochrome layer. In the presence of the chloride ion and in excess of CO_2 or in the presence of the HCO_3^- and CO_3^{2-} anions, azurite ($Cu_3(OH)_2(CO_3)_2$) *ceruzite* ($Pb_2(OH)_2CO_3$) and other basic or oxihydroxide carbonates form in certain areas. Similarly, in the presence of the SO_4^{2-} anion there result compounds of the series: *chalconite* ($CuSO_4 \times 5H_2O$),

antlerite ($Cu_3(OH)_4SO_4$), *brocantite* ($Cu_4(OH)_6SO_4$) *and/or langite* ($Cu_4(OH)_6SO_4H_2O$), *etc.* [8-26].

The appearance of aging cracks and pitting corrosion often allows the chloride anion and the oxygen in the air, water or moist soil to activate the surface of the item under the primary patina, there forming a series of very reactive Cu(II) complex compounds that penetrate the primary patina to the surface, growing into crystallite shapes, bulbs or lumps, also named *carbuncles* [8, 15-26]. Those formations then develop on larger areas, engulfing other cationic species by mineralization, thus forming the secondary patina [15-30].

Secondary patinas frequently appear as well formed microstructures and crusts on the exterior (with or without crystallite jolts), mono- or polychrome, such as: foiled structures, flat lumps or bulbs, structures resembling alveoli, separated or not by networks of cracks.

The bronze items that were kept in open spaces, in conditions of high humidity and in the presence of certain corrosion gases, there occur processes of solvolysis of those compounds, which result in widened pits that preserve unaltered inside them the layers of cuprite or chalconite (fig. 1) [2, 5, 6, 8, 11-26].

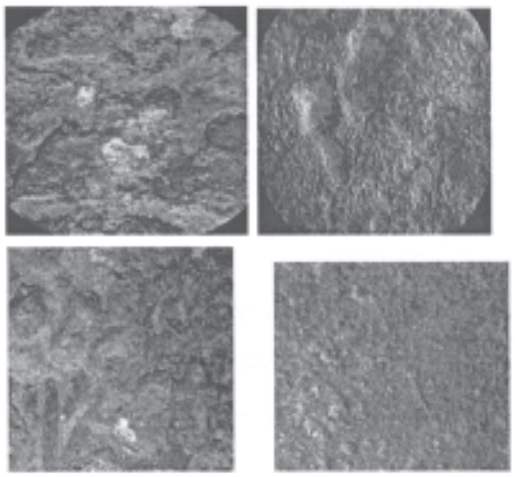

Fig. 1. Surface effects on bronze coins dated 1880-1888 preserved in time in an atmosphere with varied humidities [5, 6]

Thus, certain coins from the 17th - 19th centuries that were made by punching, displayed some rarely encountered surface effects (fig. 1). Apart from the effects that were shaped as flat lumps or bulbs, they also displayed effects of dislocation or peeling, caused by processes of dissolution, resulting in widened pits, round or oval, the bottom of which contained only one of the stable compounds that form the primary patina (cuprite, tenorite or malachite). Moreover, on a series of coins, we observed irregular patterns in the cuprite coating, crystallized microstructures - randomly developed on small areas, cuprite or malachite foils, microlumps and alveoli, cellulitic structures, flat dendritic patterns, or "orange peel" structures.

The secondary patina often features beautifully structured crystallized patterns on the surface of the crusts or in the pits of the surface formations.

Certain bronze items, with a higher concentration of tin, which had been insufficiently processed, develop a separation of small lens from those metals that are less active than the zinc or iron in their composition, the electrochemical potential thereof leading to their segregation toward the surface of the metallic core, where they dissolute and disperse into the soil, carried by water, thereby impoverishing the basic alloy. The small Sn and Pb lens may be found on the surface of the core, under the coating of cuprite or chalcolite that conserves them, but also beyond that, which seems to demonstrate that the aggressiveness of a site leads to the structural reformation thereof, under the influence of seasonal factors (fig. 2).

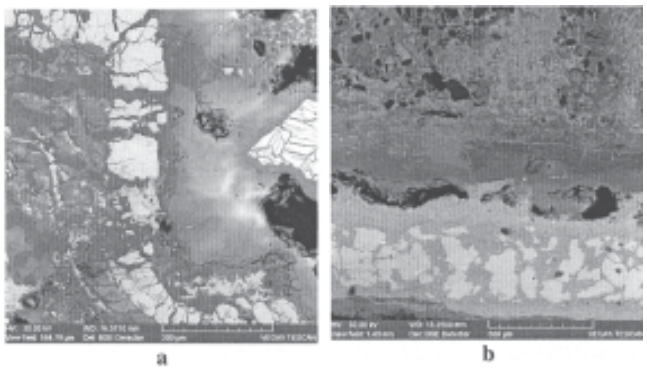

Fig. 2. The presence of lead and tin lens in the stratigraphical structure of the corrosion bulk: a - below and above the protective coating of Cu_2S and Cu_2O on the surface of the metallic core; b - under the nantokite coating between the corrosion bulk and the metallic core [11]

The concentration of iron, zinc and other active metals (from the far left side of the electrochemical series) in ancient bronze and brass alloys is considered an important archaeometric characteristic [4]. The catalyst in those processes is the chloride anion, which, by having a very small volume, migrates through fine cracks and orifices, corroding the basic alloy, in the presence of highly oxidized cations and of the diffused oxygen [4, 15-26]. The protective capacity of the ceram calcogenic coatings from the Cl^- anion is directly proportional to the *relative molar volume* of the corrosion compound in that particular coating, in direct correlation with the epitaxial relation between the growth of the crystals in the coating and the crystalline orientation of the metallic core below it [10].

The tertiary, or contamination patina forms during the underground stay period, as a development of the secondary patina, which incorporates certain microstructures from its surroundings into the surface of the object, through processes of levigation, mineralization and monolithization [15-26]. The tertiary patina appears as monolithic bulks, with or without a metallic core, containing microstructures of plant or animal fibers, insects etc., integrated into their surface. Those microstructures integrated into the bulk by contamination from the archaeological site are of great importance in any archaeometric study, as they reveal details from various stages in the evolution of an item. Currently, the archaeometry of the bulk is in need of fresh approaches in regard to the identification of structural components and the clarification of the formation/absorption mechanisms.

For instance, the bulks of certain coins and of other Byzantine bronze items from the 9th-12th centuries, which were extracted from the Nufărul and Novium-Dunum sites, in Tulcea county, contain remains of wood in their monolith (fig. 3). This picture presents the cross-section image of two bronze coins that contain partially conserved wood fragments.

The SEM-EDX analysis performed on the circled areas 1, 2 and 3 from figure 3b, confirmed the presence of partially burned wood, with visible dendrological elements (micro-fibers and growth rings), from the abandonment phase of the item. It seems that the coins were abandoned while hidden in a wooden box whose fragments got conserved by the Cu(II) compounds, during their underground stay.

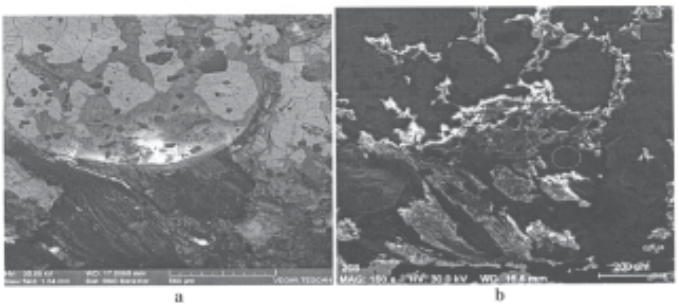

Fig. 3. SEM image of a cross-section of bronze coins (10th century), in which we can see the partially conserved wooden structures [1, 11]: a - the location of the wood fragment between the metallic core and corrosion bulk b - areas with monolithized fragments, between the core and the bulk, which under analysis revealed the presence of old wood, from the abandonment phase of the item

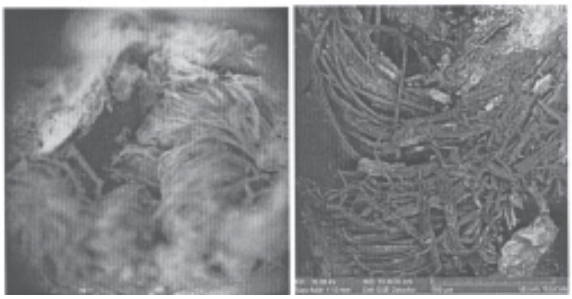

Fig. 4. Mineralized textile structures in the corrosion bulk, with a well conserved morphology [15, 16]

Textile materials, monolithized in the structure of the corrosion bulk are rare (fig. 4) and so are other organic structures (leather, bone etc.) that were conserved in sites undisturbed by pedological processes [15-26].

The interest of investigators and restorers is in clarifying the formation mechanism for the three patinas and their distribution in the corrosion crust, which would allow them to evaluate specific archaeometric characteristics and establish optimal preservation-restoration procedures.

The Elucidation of the Formation Mechanism for the Liesegang Effect

One very important archaeometric aspect, common to many archaeological bronze items, is the Liesegang effect, which appears both in items with and in those without a metallic core. The problem that keeps researchers wondering is the formation mechanism for the layered ring structures in the section of the corrosion bulk, which is dictated by the aggressiveness and the cyclical factors of the surrounding environment and also by the composition of the alloy and the conservation state of the item on its abandonment [1, 15, 16].

Such structures were the subject of studies made by many researchers [10, 15-26], of systematic PhD papers [11-14, 31] and of projects funded by the EU [32].

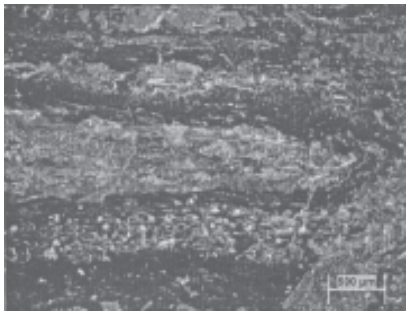

Fig. 5. Micro-photography of a sample bronze coin from Nufărul, cross-section by OM, Light Field: overview (50X)

In most of the bulks with concentric layered structures, especially in those without a metallic core, the center of the bulk is a gray compound, surrounded by a very thin layer of nantokite, followed by a thicker red cuprite layer, then by a thin green-gray one of malachite and then the layering (more or less uniformly) repeats for several sequences with the same arrangement and toward the exterior there are black layers, alternating with green-gray and thin red layers, and even farther outwards we find once more the thick red layers, alternating with green ones etc.

A clear Liesegang stratification was visible under the microscope in a median fracture of a bronze coin found in the Nufărul archaeological site (Dobrogea-Romania). The cross-section images were taken under an optical microscope at 50X magnification of its central area (fig. 5) and similar structures were seen in a series of coins from the Ibida site (Dobrogea-Romania) analyzed by SEM at 50-100X magnifications (fig. 6), revealing the presence of concentric rings.

The cross-section image of the coin from Nufărul (fig. 5) revealed a very fragile core, with a complex composition of corrosion products, even though that site was not among the disturbed ones.

Along the Liesegang effect, a series of coins from the Ibida site (fig.6) revealed the presence of monolithized fragments of silicate, calionite, coatings of sulfite, wood, micro-fossils etc., all from the surrounding soil [1].

Thus, the metallic core is often surrounded by a black-gray layer of nantokite (fig. 6 - line I), quite compact, followed by other rings of various congruent chemical systems (as dispersions from dominant compounds, chemically or physically inserted in small concentrations with others from the item or the soil). Between those concentric layers there are complex monolithic structures resulted from contamination (fig. 6 - line II) [2, 11].

A detailed SEM-EDX analysis of the layers from the cross-section of the coin from the Nufărul site (fig.5), on the transversal vector (fig. 7a), the EDX graph of the variation in the composition of chemical elements (fig. 7b) identified cuprite by Cu (red), nantokite by Cl (yellow), malachite by C (blue, chalcocite by S (orange), starting from the metallic

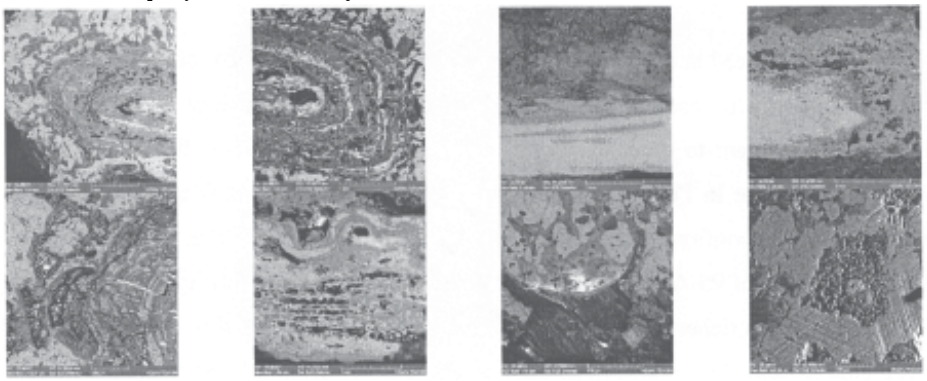

Fig. 6. SEM cross-section images (50-100X) of bronze coins (10th century): the first row shows the Liesegang effect in those from an undisturbed site; the second row shows complex monolithic structures with silicates, calionite, sulfite coatings, wood, micro-fossils [2]

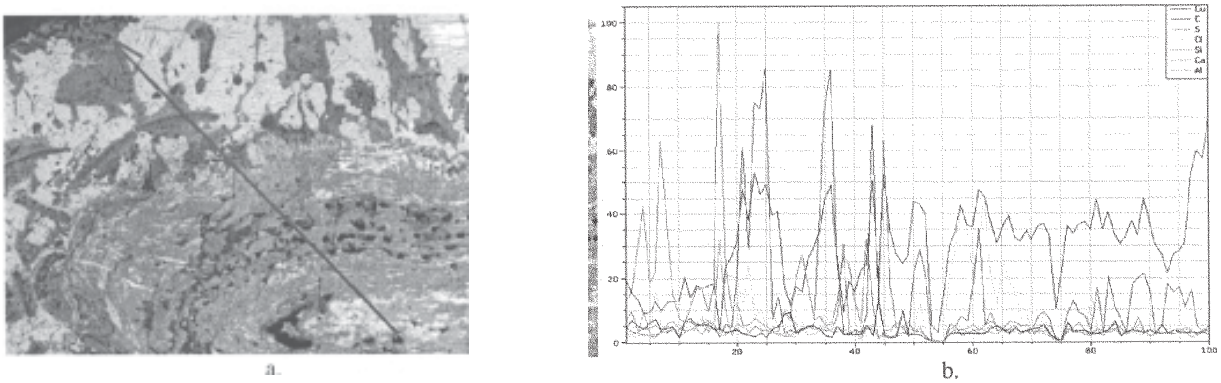

Fig. 7. The SEM microphotogram and the EDX spectrum along the vector of component element variation for the coin in figure 8, magnified to 300X [2, 11]: a - detail of the chosen vector; b - variation in Cu concentration (red), C (blue), S (orange), Cl (yellow), Si (magenta), Ca (green), Al (cyclam)

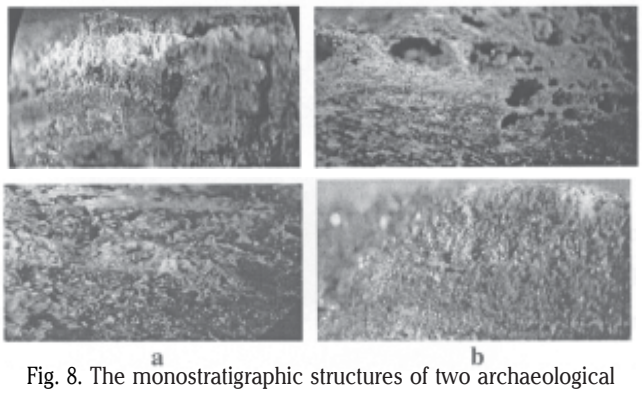

Fig. 8. The monostratigraphic structures of two archaeological bulks of bronze [1, 5, 6]: a - undisturbed site with low humidity, b - disturbed, highly aggressive site with a surplus of phreatic water

core and along the Liesegang rings. Toward the exterior there is a domination of contamination elements.

Figure 8 reveals the discontinuity in the exterior layers of the stratigraphic section under the influence of pedological disturbances (disturbed site) and of the cyclical aggressiveness of the surrounding environment, primarily of humidity and soil temperature and of the accessibility of atmospheric oxygen [1, 5, 6].

Figure 9 reveals a novel stratification in a bronze pin, cracked longitudinally, from the Ibida site, its cross-section presenting a concentric, discontinuous Liesegang effect at the level of the four cracks/pits forming a cross, which were determined by the structure resulted from the mechanical processing during its manufacture, but also by the aggressiveness of the seasonal, dry/wet cycles. Interestingly, all the fragments uncovered in the site feature the same disposition of the pits resulted by cracking and the same discontinuity of the corrosion products from the surface, very precisely differentiated into specific types of (chemically congruent) compounds: nantochite, cuprite, casiterite, azurite, malachite etc.

A similar effect was recently observed in a series of round antique bronze items, from the Haft Tappeh archaeological site, in the south-west of Iran, which featured a similar radial cracking system (fig. 10) and were studied by Omid Oudbashi and others [31].

The SEM-EDX results from the items found in Iran are very close to the ones we obtained from our items with the Liesegang effect, which were found in Romania and which are presented below.

Thus, figure 11 presents the variation in the concentration of elements (Cu, Sn, O, C and Si) in the corrosion bulk of a coin found in the Ibida site (fig. 9). We performed our SEM-EDX analysis along the vector that crosses the Liesegang rings from the upper right arm of the cross-sections (fig. 9b and 11a). While copper presents an almost constant cyclical variation on each ring, tin has two concentrations: a higher one on the rings in which the oxygen concentration is null and a medium one, close to the concentration of oxygen, in the other rings. Chlorine and silicon have very low and constant concentrations, which demonstrates that the aggressiveness of the surrounding environment had a constant cycle, a low concentration of chloride anions and a weak monolithic contamination (fig. 11b).

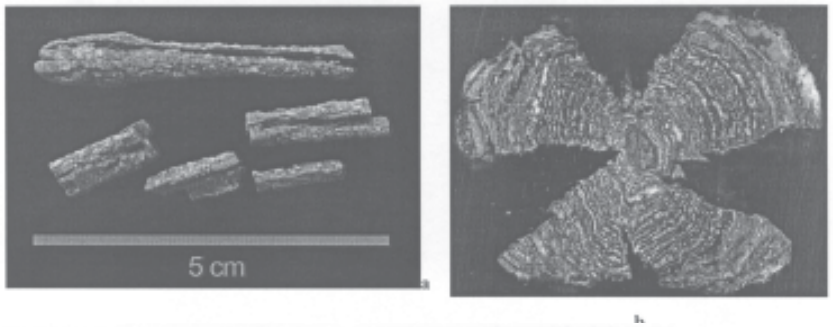

Fig. 9. Fragments of a safety pin discovered in Ibida (Dobrogea) (a) and Stereomicro-photography of sample's cross-section, Dark Field: overview (50X) of one of the fragments (b) [1, 11]:

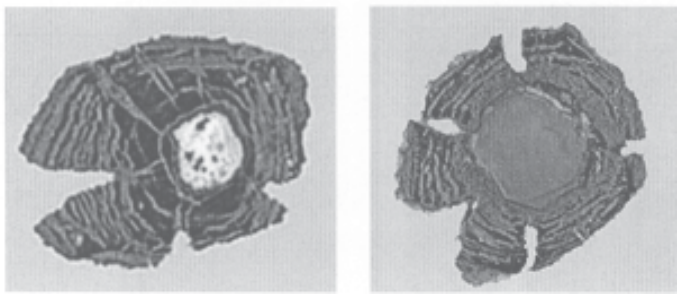

Fig. 10. Microphotogram of a cross-section from two items from Haft Tappeh, S-E Iran [31] a - The multilayer structure of red-brown huge corrosion phase and white-grayish phase are visible b - The white-grayish phase is visible in center this sample. The red-brown corrosion layer has some cracks that continued into the inner part of the sample

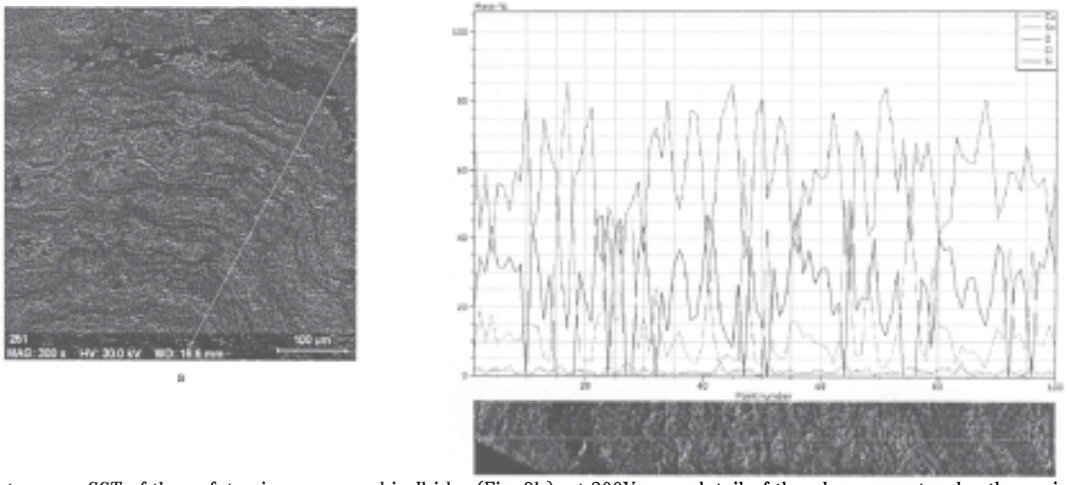

Fig. 11. SEM Microphotogram -*SST* of the safety pin uncovered in Ibida (Fig. 9b), at 300X: a - detail of the chosen vector; b - the variation in the concentration of Cu (red), Sn (green), O (blue), Cl (cyclam) and Si (magenta), along the vector [1, 11]

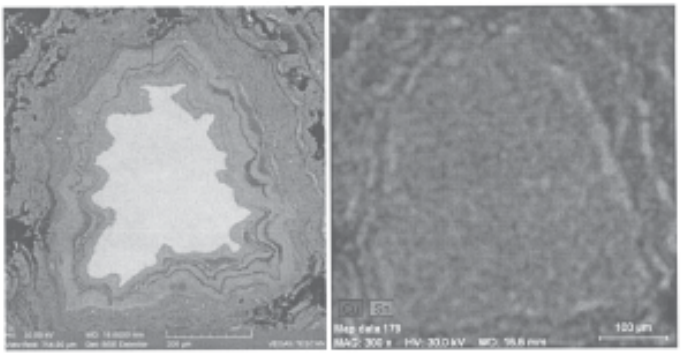

Fig.12. Detail from the core of the item in figure 12. Arrangement of layers of tin, responsible for generating coatings hydrogels leading to Liesegang effect. Comparison between BSE micrograph and image reporting the overlapping Cu-Sn showing the segregation of cuprite and cassiterite [1, 11]

Figure 12 details the layered structure of the central area from the item in figure 9b, obtained by SEM-EDX, with the displacement of the main compounds (a) and the mapping of the chemical elements thereof (b), highlighting the differentiated distribution of the main two alloy compounds, Cu (red) and Sn (green), both in the metallic core and in the first Liesegang rings. This figure reveals a decrease in the tin from the metallic core and its segregation outwards, and at the surface of the core the existence of a thick coating of tin-based compounds, followed by successive layers of copper and then of tin-based compounds, clearly differentiated into structures of chemical congruent elements based on nantokite, atacamite, malachite, azurite etc., each separated by cuprite rings.

This example explains the formation of the Liesegang rings, by involving the compact Sn(IV) hydrogels coating agents from the surface of the core and implicitly the formation of those that occur between the successive rings of tenorite and cuprite.

Another example that revealed the concentration of tin, present in compounds, on the surface of the basic metal is that of an item found in 2008 Nufărul (Dobrogea), in an undisturbed site, which allowed it to remain well conserved [1, 11-14]. A SEM-EDX analysis of a cross-section (fig. 13) clearly revealed the concentration of tin on the surface, followed by a corrosion layer, impregnated with monolithized components from the soil (silicates). At this interface the silicates are precisely delimited (compact layer) with weak signs of penetration from the site in the volume phase of the corrosion products that are based on tin oxides and chlorides, the compounds that form protective coatings during the underground stay of an item.

Figure 14 reveals the Liesegang structure in the cross-section of a pin found in Ibida, which had a very well

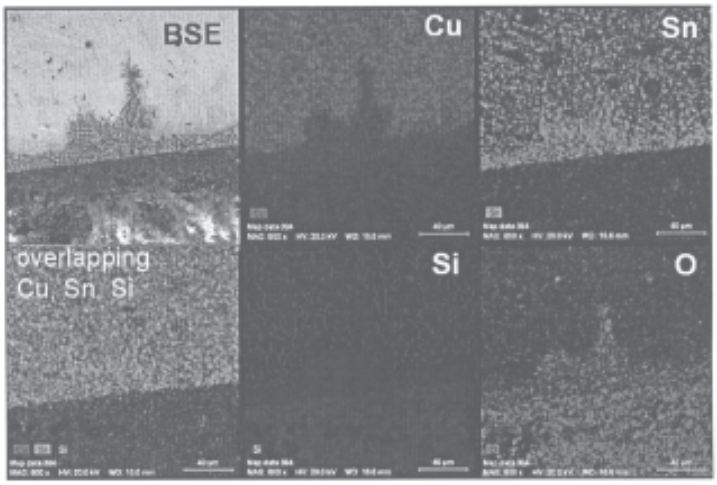

Fig. 13. SEM-EDX mapping showing the elemental distribution of Cu, Sn, Si and O in the corrosion layers (800X) [11]

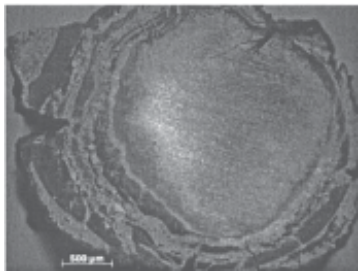

Fig. 14. Microscopic image of the cross section of a pin (50X) [1, 11]

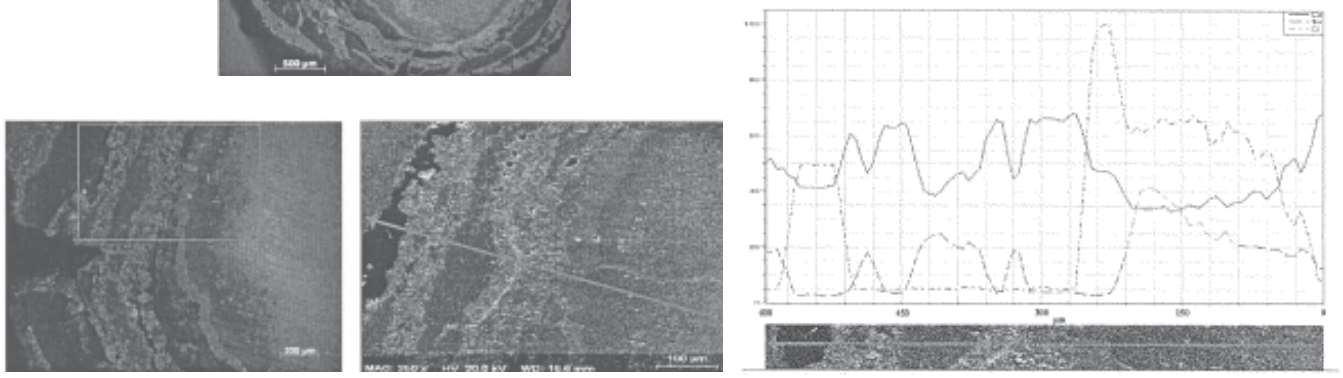

Fig. 15. Element Profile Obtained by EDX-line scan [1, 11]: distribution of Cu, Sn and O: a – detail microscopic image (Fig. 14); b – analysis vector and c – variation of the Cu, Sn and Cl concentrations along the vector

Table 1
VARIATION OF THE RATIO BETWEEN THE CONCENTRATION OF CU/SN ALONG THE 8 LIESEGANG RINGS SHOWN IN FIGURE 16

No. of Liesegang Ring	0	1	2	3	4	5	6	8
Cu/Sn Ratio atomic %	10.00	0.65	2.63	9.09	5.26	100.00	4.17	33.33

preserved metallic core, with a distribution similar to that of the corrosion compounds in the concentric layers and of the pits resulted from dehydration. Around the metallic core, with a high concentration of tin and lead (matte-gray) on the outside, there is a very thin layer of casiterite (bright dirty-white), followed by cuprite (brown-red), cuprite inserted in covellite (violet-blue), then there is a thin layer of malachite (green), followed by similarly successive layers until the surface of the crust.

The EDX data in figure 15 confirm a decrease in the concentration of copper, from the center of the metallic core to the first nantokite layer coating its surface, and an increase in the concentration of tin and chlorine.

Before the first layer of nantokite, turned into casiterite, there is a fine coat of a hydrogel based on Sn(IV) of 10μm and outwards, above this layer, the high concentration of copper indicated the presence of a cuprite layer of 30μm and then the concentration decreases, as that of tin increases for app. 20-30μm and then there is a cuprite layer of app. 25-30μm, covered by a 20μm thin one of nantokite.

Table 1 presents the variation of the ratio between the concentration of Cu/Sn, corresponding to the vector that crosses the Liesegang rings shown in figure 15b. The rings were delimited and numbered 1 to 8, from the core outwards (fig. 16). The figure also presents the areas selected for SEM-EDX analysis. We should mention that the metallic core was well conserved.

The SEM-EDX analysis of the gray-white metallic cores shown in figure 15 and 16, correlated with similar analyses performed on other items with Liesegang rings and a fragile core, shows that in the center they contain a large quantity of copper (84.3%), mixed with tin (12.5%) and very little chlorine (3.2%), which decreases toward the surface of the core, where the quantity of tin increases to app. 72% and that of copper decreases to 10%, the chlorine reaching 8%. At the intermediary rings between the metallic core and the first layer of cuprite (ring 5, fig. 16), with a Cu/Sn ratio of 100, the concentration of copper slightly increases

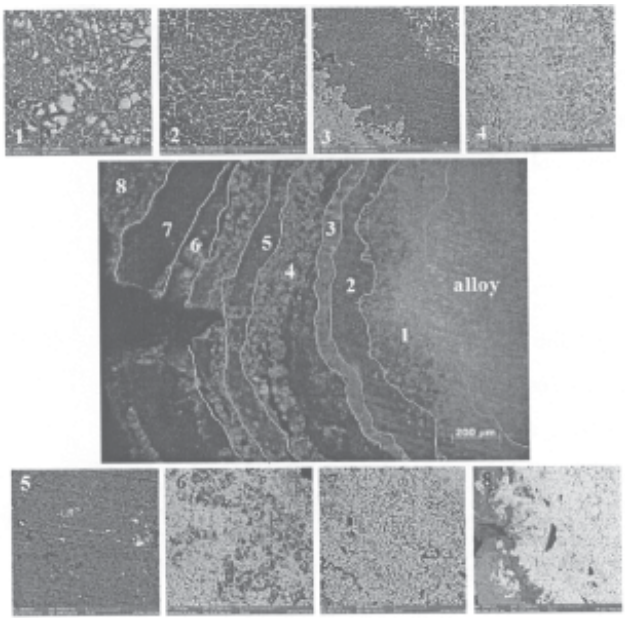

Fig. 16. The SEM microphotographs in cross-section of the 8 Liesegang rings analyzed by EDX [1, 11]

to the detriment of tin (12.3%), oxygen (22%) and increased chlorine, especially in rings 2 and 3 (app. 18% Cl). In the items that contain lead, its variation in composition follows a pattern close to that of tin. Nevertheless, the analysis of the brown-red layer around ring 5 (rings 4, 5, and 6), based on cuprite, inserted between the violet-blue CuS layer (rings 3 and 6) and the nantokite layers (rings 2 and 7), indicated a high content of Cu (76%) and oxygen (10%) and a low content of Sn/Pb(6%), S (5%) and Cl (3%). The green malachite structures are rich in copper (62%) and oxygen (22%), with very low and variable concentrations of Sn/Pb and Cl.

Towards the exterior layers the concentration of chloride decreases and that of carbonate, sulfate etc. oxyanions increases, while the Sn/Pb concentration decreases proportionally to that of copper. There we often identified

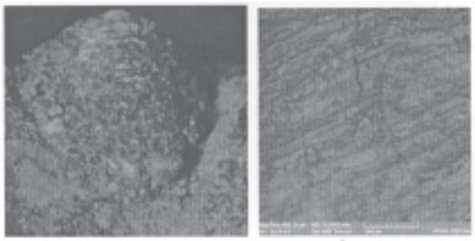

Fig. 17. Discontinuous forms of Liesegang effect with film-forming hydrogels and concentric distribution to a rivet of the same material with the support, revealed at the surface: a – optical microscope image (50X), b – SEM image (300X) [15, 16]

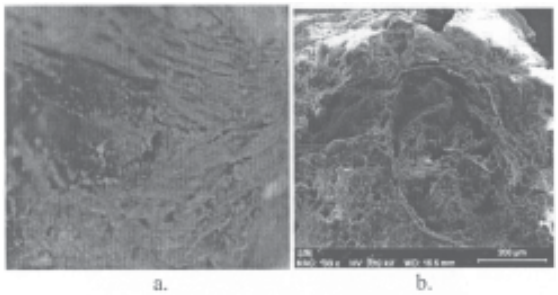

Fig. 18. Discontinuous forms of Liesegang effect with film-forming hydroxy and chloride based apatite [15, 16]: a - Honeycomb membranes of chlorapatite remaining after removal of the Liesegang stratified compounds; b - SEM image of Liesegang stratified compounds, with honeycomb membranes of hydroxyapatite partially empty (200X)

anhydrous and hydrated Cu(II) sulfates (*chalconite* - $CuSO_4 \times 5H_2O$, *antlerite* - $Cu_3(OH)_4SO_4$), *brocantite* - $Cu_4(OH)_6SO_4$ *and langite* - $Cu_4(OH)_6SO_4 \times H_2O$). Some items without a metallic core often contain other thick layers of malachite ($Cu_2(OH)_2CO_3$) toward the exterior and in certain areas there were crystallites of *azurite* ($Cu_3(OH)_2(CO_3)_2$).

Figure 17 presents an atypical case of Liesegang effect, formed with the aid of semi-membrane hydrogels, which was identified on a fragment from the rim of a shield found in Văleni, Neamt county (Romania) [15, 16]. It is a Liesegang effect that developed concentrically in an area, as a bulb and did not extend over the entire item.

Figure 18 presents another atypical case of Liesegang effect, which developed by continuous processes of crystalline reformation, under the influence of membrane systems of the chloride/hydroxyapatite type, that were identified on a bronze item found in Gabăra, Neamt county (Romania). That type of Liesegang effect contains membranes of chloride and hydroxyapatites grown in a honeycomb pattern, empty, or partially so, after the dissolution of the compounds in those layers [15, 16].

The Liesegang structures above (fig. 17 and 18) formed by two different mechanisms in the presence of some thin layers of hydrogels based on oxyhydroxides of metals (Sn, Pb and Zn) and on chloride- or hydroxyapatite-based coating agents. The first mechanisms conserve the Liesegang stratification, as hydrogels are membrane systems only affected by direct osmosis, whereas the others are not, because chloride- or hydroxyapatites form systems which are affected by direct and inverse osmosis and they allow the dissolution of the layered compounds and their shift into the water in the soil, the only remains being structures with honeycomb patterned cavities. An important role is obviously played by the aggressiveness of the soil and by the cyclical factors during the underground stay of an item.

Conclusions

The archaeological bronze items that do not contain any residual metallic core raise some very important and complex problems in regard to their authentication. Such items are often destined for the 'grey fund' and abandoned, in most cases, during preliminary selection, immediately after excavation. Those items can be a very important source of information, mainly about the basic alloy and often as unique proofs of a specific technique or metallurgical tradition/period. In that regard, our research presents the three structural components of the archaeological patina identified in the section of the corrosion bulk of bronze items, namely: *primary* or *noble patina* (oxides, sulfurs etc.), resulting from chemical (dry environment) and/or electrochemical (humid environment) redox processes, formed during the period of manufacture and during use of an object, *secondary,* or *poor patina* – appearing in the final stage of use and continuing into the early, after abandonment stage, by redox and coordination processes, assisted by acid – base processes, by ion exchange, hydrolysis (oxihydroxides, halogens, carbonates, sulphates, phosphates etc.) and/or thermal (calcination, recrystallization etc.) and the last patina, the *tertiary* or *contamination patina*, formed in the archaeological site under the influence of soil/pedological processes (segregation, diffusion, osmosis/electro-osmosis, monolithization, dissolution/recrystallization, hydration/dehydration etc.).

The three types of structures are present in items coming from both disturbed and undisturbed sites.

These forms are of different typologies, according to their extension, morphology and stratification, depending on the nature of the coating that formed (hydrogels and hydroxyapatite), on the composition of alloys and also on the soil aggressiveness and on site conditions.

References

1 SANDU, I., Degradation and Deterioration of the Cultural Heritage**,** Vol. 1, "Al.I.Cuza" University Publishing House, Iaşi, 2008, p. 187-276.
2. SCOTT, D.A., J. American Institute for Conservation, **29**, 1990, p. 193.
3. SANDU, I., DIMA, A., SANDU, I.G., Restauration and Conservation of Metallic Artefacts, Ed. Corson, Iaşi, 2002.
4. SCOTT, D.A., Corrozion, Colorants, Conservation, Ed. The Getty Conservation Institute, Los Angeles, 2002, p. 164.
5. SANDU, I., URSULESCU, N., SANDU, I.G., BOUNEGRU, O., SANDU, I.C.A., ALEXANDRU, A., Corrosion Engineering Science and Technology, **43**, no. 3, 2008, p. 256.
6. SANDU, I.G., STOLERIU, S., SANDU, I., BREBU, M., SANDU, A.V., Rev. Chim. (Bucharest), **56**, no. 10, 2005, p. 981
7. BERTHELOT, M.P.E., Comptes Rendus Hebdomadaire des Seances de l'Academie des Sciences, **188**, 1994, p. 768;
8. ROBBIOLA, L., BLENGINO, J.M., FIAUD, C., Corrosion Science, **40**, no. 12, 1998, p. 2083.
9. CONSTANTINIDES, I., ADRIAENS, A., ADAMS, F., Applied Surface Science, **189**, 2002, p. 90.
10. MAZZEO, R., Le patine. Genesi, significato, conservazione – Kermesquaderni, Ed. Nardini, Firenze, 2004, p. 29.
11. QUARANTA, M., SANDU, I., On the Degradation Mechanisms under Infuence of Pedological Factors through the Study of Archaeological Bronze Patina, "Al.I.Cuza" University Publishing House, Iaşi, 2010.
12. QUARANTA, M., SANDU, I., *Proceedings of the ART 2008-9*, Ed. ISAS, Jerusalem, 2008, Paper no. 147, www.ndt.net/article/art2008/papers/147Quaranta.pdf.
13. QUARANTA, M., SANDU, I., 37th International Symposium on Archaeometry, Fondazione Monte dei Paschi di Siena, Italy, 2008, p. 421.

14. QUARANTA, M., CIOCAN, A.C., SANDU, I., 5th International Conference on the application of Raman Spectroscopy in Art and Archaeology, Bilbao, Spain, 2009, p. 182.
15. SANDU, I.G., MIRCEA, O., VASILACHE, V., SANDU, I., Microscopy Research and Technique, **75**, no. 12, 2012, p. 1646.
16. MIRCEA, O., SANDU, I., VASILACHE, V., SANDU, A.V., Microscopy Research and Technique, **75**, no. 11, 2012, p. 1467.
17. VASILACHE, V., BOGHIAN, D., CHIRCULESCU, A.I., ENEA, S.C., SANDU, I., Rev. Chim. (Bucharest), **64**, no. 2, 2013, p.152.
18. APARASCHIVEI, D., VASILACHE, V., SANDU, I., International Journal of Conservation Science, **3**, no. 1, 2012, p. 23.
19. SANDU, I., MIRCEA, O., SANDU, A.V., SARGHIE, I., SANDU, I.G., VASILACHE, V., Rev. Chim. (Bucharest), **61**, no. 11, 2010, p. 1054.
20. MIRCEA, O., SANDU, I., VASILACHE, V., SANDU, A.V., Rev. Chim. (Bucharest), **63**, no. 9, 2012, p. 893.
21. VASILACHE, V., APARASCHIVEI, D., SANDU, I., International Journal of Conservation Science, **2**, no. 2, 2011, p. 117.
22. SANDU, I., APARASCHIVEI, D., VASILACHE, V., SANDU, I.G., MIRCEA, O., Rev. Chim. (Bucharest), **63**, no. 5, 2012, p. 495.
23. MIRCEA, O., SANDU, I., SARGHIE, I., SANDU, A.V., International Journal of Conservation Science, **1**, no. 1, 2010, p. 27.
24. SANDU, I., MIRCEA, O., SARGHIE, I., SANDU, A.V., Rev. Chim. (Bucharest), **60**, no. 10, 2009, p. 1012.
25. MIRCEA, O., SARGHIE, I., SANDU, I., URSACHI, V., QUARANTA, M., SANDU, A.V., Rev. Chim. (Bucharest), **60**, no. 4, 2009, p. 332.
26. MIRCEA, O., SARGHIE, I., SANDU, I., QUARANTA, M., SANDU, A.V., Rev. Chim. (Bucharest), **60**, no. 2, 2009, p. 201.
27. SANDU, I., SANDU, I.C.A., Egyptean Journal of Archaeologycal and Restoration Studies, **3**(2), 2013, p. 73.
28. SANDU, I., MIRCEA, O., SANDU, I.G., VASILACHE, V., International Journal of Conservation Science, 4(SI), p. 573.
29. MIRCEA, O., SANDU, I., VASILACHE, V., SANDU, A.V., International Journal of Conservation Science, 4(SI), p. 701.
30. VASILACHE, V., SANDU, I., MIRCEA, O., SANDU, A.V., International Journal of Conservation Science, 4(SI), p. 710.
31.OUDBASHI, O., MOHAMMADAMIN EMAMI, S., AHMADI, H., DAVAMI, P., Heritage Science, **1**, 2013, Paper no. 21, http://www.heritagescience journal.com/content/1/1/21.
32. *** EFESTUS European Project, INCO-MED Contract No. ICA3-CT-2002-10030 (www.efestus.just.edu.jo/index.jsp)

Manuscript received: 11.11.2013